Fourth International Conference on CFD in the Oil and Gas, Metallurgical & Process Industries
SINTEF / NTNU Trondheim, Norway
6-8 June 2005

A MODEL OF THE FLOW OF GRANULAR MATERIALS DOWN CHUTES

Mohamed SAYED[1] and Stuart B. SAVAGE[2]

[1] Canadian Hydraulics Centre, National Research Council, Ottawa, Ontario, CANADA
[2] Department of Civil Engineering and Applied Mechanics, McGill University, Montreal, Quebec, CANADA

ABSTRACT

This paper develops models and constitutive equations that are intended for the calculation of granular flows down inclined channels. The flows are assumed to involve fairly large particles at high concentrations. Furthermore, it is assumed that the flows are rapid, and that the particle velocity fluctuations are vigorous. We make use of results derived from the kinetic theories of granular flows to develop simplified expressions that can be used to determine stresses, and velocity and density profiles in channelized flows. The paper focuses on the particle collisional stress contributions, but the effects of the 'frictional' stresses that come from the enduring interparticle contacts are also considered. A solution for steady uniform flow is also presented. The results are verified through comparisons to a few available experimental measurements. The comparisons indicate that predicted velocities and flow rates are close to the experimental measurements.

NOMENCLATURE

a, b coefficients in Equation (10)
a_c average boundary area per particle
$\boldsymbol{C}$ velocity fluctuations
$\boldsymbol{c}$ instantaneous velocity
d_p particle diameter
e coefficient of restitution
g gravitational acceleration
g_0 radial distribution function
h flow depth
k_1 function of solids volume fraction
k_2 function of solids volume fraction
N_f quasi-static normal stress at the boundary
R parameter (Savage-Jeffrey number)
S_f quasi-static shear stress at the boundary
T granular temperature
s distance between centre of a particle and the boundary
$\boldsymbol{u}$ velocity vector
u,v components of the velocity vector
u_{sl} slip velocity at the boundary
u_{wall} velocity of the boundary
α coefficient in Equation (10)
δ angle of friction between the boundary and the bulk particles
η parameter in Equation (1)
φ_d dynamic angle of internal friction
φ_f quasi-static angle of internal friction
φ' specularity coefficient
ν solids volume fraction
ν_{max} maximum solids volume fraction
ν_{min} minimum solids volume fraction
ρ bulk density
ρ_p particle density
σ stress tensor
σ_{ij} components of the stress tensor
i,j indices of the stress tensor components
x,y indices indicating x and y directions

INTRODUCTION

The focus of this paper is on dense granular flows down chutes. In particular, we consider two-dimensional flows with the main component of the velocity along the streamwise direction, and with small transverse velocity components by comparison. Our goal is to develop simple expressions for the stresses that can be used in future numerical solutions of more complex flow conditions. The aim is make approximations to achieve simplicity and ease of programming, at the expense of what are hoped to be minor losses of accuracy and generality.

In the flow regime of present interest, a velocity profile develops within the granular material, with a possible slip velocity at the frictional base of the chute. Importantly, those flows can reach steady fully developed states for a range of slopes. Johnson et al. (1990) considered such flow regimes to be governed by both frictional and collisional interactions between the particles. The frictional stresses were considered to be rate independent. The collisional stresses represented the rate-dependent and can be modelled by *kinetic theories* (Lun et al., 1984). Johnson et al. (1990) employed a simple superposition of the two types of stresses to obtain a solution of the fully developed flow, which successfully reproduced expected flow patterns.

The introduction of kinetic theories or dynamic stresses requires the determination of the *granular temperature*, which is a measure of the energy associated with velocity fluctuations. This, in turn, is usually based on solving an energy balance equation that describes the evolution of granular temperature. In the following sections of the paper, we develop a simple expression for the dynamic stresses. Consequently, solving the complex granular temperature equation can be avoided. We then develop a solution for the flow down a chute based on the new simplification.

STRESSES DEVISED FROM GRANULAR FLOW KINETIC THEORIES

In dealing with granular flows, it is common to separate the contributions to the stresses into three parts. The first is the so-called kinetic contribution that in a shear flow results from the transport of momentum as particles move from one shear layer to an adjacent one. This is the mechanism that gives rise to viscosity in a dilute gas. The second contribution to the stresses comes from the interparticle collisions; at high concentrations and rapid shear rates this makes up a major part of the total stresses. Finally, there is a so-called quasistatic contribution that arises from particles involved in enduring contacts overriding one another.

We shall develop simple expressions for the stresses based on (i) granular flow kinetic theories, and (ii), assumptions about the connection between shear rates and the granular temperature that is proportional to the mean square of the particle velocity fluctuations. By this means we can avoid the explicit use of the granular temperature evolution equation that is an equation for the development of kinetic energy of the velocity fluctuations. These results are not appropriate for general flow fields, but should be regarded as approximations that may be used for essentially uniaxial flows down chutes.

Dynamic Stresses

We develop, in this section, simple expressions for the dynamic (kinetic and collisional) stresses. We begin by defining the sign convention that will be used for the stresses. As shown in Figure 1, normal compressive stresses are considered positive. Directions of the positive shear stresses are also shown in the sketch.

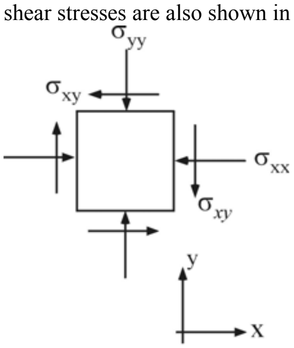

Figure 1: Sign convention for normal and shear stresses.

Consider a two-dimensional granular flow in which the primary velocity is the *u*-component oriented in the streamwise x-direction. The velocity component *v*, that is oriented in the y-direction, perpendicular to the bed, is assumed to be small, i.e., $v \ll u$. We also assume that the velocity gradients in the y-direction are much greater than those in the streamwise x-direction. Thus, of the six gradients of the velocity components, $\partial u_i/\partial x_j$, where i =1,2 and j=1,2, the dominant component is $\partial u/\partial y$.

Making use of the granular kinetic theory results of Lun et al. (1984), the total normal stresses, consisting of the sum of kinetic and collisional stresses, are approximated by

$$\sigma_{xx} \approx \sigma_{yy} \approx \sigma_{zz} \approx \rho\left(1 + 4\eta\nu g_0\right)T \qquad (1)$$

where $\rho = \rho_p\ \nu$ is the bulk particle density, ρ_p is the mass density of the individual particles, ν is the solids fraction, $\eta = (1 + e)/2 \approx 1$, e is the coefficient of restitution, and g_0 is the Carnahan & Starling radial distribution function given in Lun, et al. (1984) as

$$g_0 = \frac{(2-\nu)}{2(1-\nu)^3} \qquad (2)$$

and $3T/2 = \langle C^2 \rangle /2$ is the specific translational kinetic energy, *T* is the granular temperature and **C** = **c** −**u** where **c** is the instantaneous velocity of the particle and **u** =< **c** > is the mean or bulk velocity. We note that there are alternative expressions for the radial distribution function. For example, Lun and Savage (1986) proposed the following expression for shearing flows

$$g_0 = \left(1 - \nu/\nu_{\max}\right)^{-2.5\nu_{\max}} \qquad (3)$$

where ν_{max} is the maximum solids fraction that will allow shearing motion to occur. Note that when $\nu \to \nu_m$ then g_0, and hence, the expressions for the stresses will diverge, corresponding to a locked system of particles. Another expression also used by Lun and Savage (1987)

$$g_0 = \frac{1}{\left[1 - \left(\nu/\nu_{\max}\right)^{1/3}\right]} \qquad (4)$$

Values of g_0 given by Equations (3) and (4) are not very different except when $\nu \to \nu_m$. Those equations are probably preferable to the Carnahan and Starling expression (Equation 2).

In certain examples of granular shearing flows, it is found that *R*, the parameter called the Savage-Jeffrey number (Savage & Jeffrey, 1981), is approximately constant and of order unity, i.e.

$$R = \frac{d_p}{T^{1/2}}\left[\frac{\partial u}{\partial y}\right] \qquad (5)$$

where d_p is the particle diameter and $\partial u/\partial y$ is the shear rate. Making the approximation that $R \approx$ constant for the present work on inclined chute flows permits us to dispense with the particle fluctuation energy equation when solving for the granular flow field. Let us make some physical observations about the assumption of $R \approx$ constant. If we neglect the fluctuation energy flux divergence in the kinetic theory granular temperature evolution equation (Lun, et al., 1984; Johnson, et al., 1990), then for a steady, fully developed chute flow, we find that there is a balance between the shear work and the collisional energy dissipation. Under these assumptions, we find that $R \approx$ constant (Lun, et al., 1984). The value of *R* depends on the dissipative properties of the particles, and very weakly on the solids volume fraction. A similar approximation has been proposed by Syamlal et al. (1993), and more recently by van Wachem et al. (2001).

If the fluctuation energy flux divergence is not zero, then the balance between the shear work and the collisional energy dissipation is not achieved and departures from a fixed value of *R* might be expected. An example of such a case is a chute flow in which there occurs a significant slip velocity at the bed, possibly generating a high granular temperature at the bed which gives rise to a flux of energy into the granular material above the bed.

Returning to the relationship between shear rate and granular temperature, we can re-arrange Equation (5) to yield an expression for the granular temperature, i.e.,

$$T = \frac{d_p^2}{R^2}\left[\frac{\partial u}{\partial y}\right]^2 \qquad (6)$$

Assuming that $\eta = (1+e)/2 \approx 1$, we can express Equation (1) as

$$\sigma_{yy} \approx \frac{1}{R^2} \nu \rho_p (1+4\nu g_0) d_p^2 \left[\frac{\partial u}{\partial y}\right]^2 \qquad (7)$$

The theory of Lun et al. (1984) shows that ratio of shear to normal dynamic stresses is roughly constant. We can, therefore, relate the shear stress σ_{xy} to the normal stress σ_{yy} through the use of a dynamic friction angle φ_d as follows, i.e.,

$$\begin{aligned} \sigma_{xy} &\approx -\sigma_{yy} \tan\varphi_d \\ &= \frac{-1}{R^2} \nu \rho_p (1+4\eta \nu g_0) d_p^2 \left|\frac{\partial u}{\partial y}\right| \left[\frac{\partial u}{\partial y}\right] \tan\varphi_d \end{aligned} \qquad (8)$$

Equations (1) and (8) can thus be used in the granular flow momentum equations to determine the profiles of mean velocity and solids fraction.

Frictional (Quasi-static) Stresses

The final contribution to the overall stresses is due to enduring contacts between the particles as they override each other at high concentrations. We simply add these quasistatic contributions to the dynamic stresses to obtain an expression for the total stresses. Johnson et al. (1990) and Anderson and Jackson (1992) have proposed a simple relation for the quasistatic stresses that is essentially a Coulomb type relationship. They relate the shear stress S_f on a shear plane to the normal stresses N_f on that plane as follows

$$S_f = N_f \sin\varphi_f, \quad N_f = N_f(\nu) \qquad (9)$$

where φ_f is the quasi-static angle of internal friction. In the present paper, however, we use $S_f = N_f \tan \varphi_f$, for algebraic simplicity. The choice of $\tan \varphi_f$ or $\sin \varphi_f$ is a matter of definition of the angle of internal friction. Care should be taken in comparing various values of φ_f quoted in the literature.

One might expect N_f to increase without bound when the solid fraction approaches its maximum value ν_{max} and particle interlocking occurs. Alternatively, when the solids fraction approaches some minimum value ν_{min}, the particles essentially lose contact with one another and the normal stress ceases to exist. Johnson et al. (1990) have proposed the following simple relationship for the ν dependence of $N_f(\nu)$

$$\begin{aligned} N_f &= \alpha \frac{(\nu-\nu_{min})^a}{(\nu_{max}-\nu)^b} \quad && for(\nu > \nu_{min}) \\ &= 0 && for(\nu \le \nu_{min}) \end{aligned} \qquad (10)$$

where α, a and b are constants. In the present paper we choose a= b= 1. From dimensional arguments, the right-hand-side of Equation (10) should take the form $\rho_p\, g\, d_p\, k_1(\nu)$, where the function $k_1(\nu)$ is dimensionless.

NUMERICAL SOLUTION

The conservation of mass and momentum equations can be expressed as

$$\frac{\partial(\rho_p \nu)}{\partial t} + \nabla.(\rho_p \nu \mathbf{u}) = 0 \qquad (11)$$

and

$$\frac{\partial(\rho_p \nu \mathbf{u})}{\partial t} + \nabla.(\rho_p \nu \mathbf{uu}) = -\nabla \boldsymbol{\sigma} + \rho_p \nu \mathbf{g} \qquad (12)$$

For the case of steady two-dimensional flow in a chute inclined an angle ζ to the horizontal (Figure 2), the above two equations reduce to

$$\sigma_{xy} = -\rho_p\, g \sin\zeta \int_y^h \nu\, dy \qquad (16)$$

and

$$\sigma_{yy} = \rho_p\, g \cos\zeta \int_y^h \nu\, dy \qquad (17)$$

Equations (7) to (10) lead to the following expressions of the shear and normal stresses,

$$\begin{aligned} \sigma_{xy} = &-k_1(\nu)\rho_p\, g\, d_p \tan\varphi_f \\ &- k_2(\nu)\rho_p\, d_p^2 \left(\frac{du}{dy}\right)^2 \tan\varphi_d \end{aligned} \qquad (18)$$

$$\sigma_{yy} = k_1(\nu)\rho_p\, g\, d_p + k_2(\nu)\rho_p\, d_p^2 \left(\frac{du}{dy}\right)^2 \qquad (19)$$

The velocity gradient (cf. Figure 2) is positive in the present case, and hence the modulus in Equation (8) is not needed in Equation (18). The functions $k_1(\nu)$ and $k_2(\nu)$ are given by

$$k_1(\nu) = \alpha \left(\frac{\nu - \nu_{min}}{\nu_{max} - \nu}\right) \qquad (20)$$

and

$$k_2(\nu) = \nu(1+4\nu g_0)/R^2 \qquad (21)$$

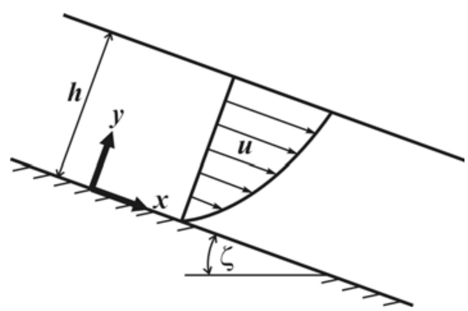

Figure 2: Sketch of flow down an inclined chute.

Equations (18) and (19) are substituted in Equations (16) and (17) to give two expressions for the unknown velocity, u and solids fraction, ν. After some manipulation, the following ordinary differential equation for the velocity is obtained

$$\left(\frac{du}{dy}\right)^2 = \frac{k_1(\nu)}{k_2(\nu)} \frac{g}{d_p} \left(\frac{\tan\zeta - \tan\varphi_f}{\tan\varphi_d - \tan\zeta}\right) \qquad (22)$$

Another algebraic equation is obtained for the solids fraction as,

$$\alpha\left(\frac{\nu-\nu_{\min}}{\nu_{\max}-\nu}\right)=\frac{\frac{\sin\zeta}{d_p}\int_y^h \nu\, dy}{\left[\tan\varphi_f+\tan\varphi_d\left(\frac{\tan\varphi_d-\tan\zeta}{\tan\zeta-\tan\varphi_f}\right)\right]} \tag{23}$$

Solution of Equation (23) was carried out using numerical integration along with an iteration scheme. Initially a mean value of the solids fraction is introduced to estimate the integral in the right-hand-side. Calculations are carried out starting at the surface, $y=h$, with the minimum value of the solids fraction, $\nu = \nu_{min}$. The integration proceeds downwards until the bed is reached, $y = 0$. At each step, an initial estimate is made of the value of ν in order to evaluate the integral on the right-hand-side of Equation (23). This procedure is repeated until changes in the profile of ν become negligible. Convergence always occurred relatively rapidly. The integration was carried out using a trapezoidal rule.

The values of ν were next used in the integration of Eq. (22) to determine the velocity distribution. Integration started from the bed ($y=0$) and proceeded upwards to the surface ($y=h$). Again, a trapezoidal rule was used in the integration. Several step sizes were also used to ensure satisfactory accuracy; step size of $\Delta y/h = 0.01$ was usually adequate.

The present solution considers two cases for the velocity at the bed. The first is a no-slip boundary condition (i.e. $u = 0$). This case would be appropriate for a rough bed surface. The second case corresponds to a non-zero slip velocity at the bed, as discussed in the following section.

Slip Velocity Boundary Conditions

An expression for the slip velocity is presented here by making use of the analysis of Johnson and Jackson (1987) and the present simplified model of the stresses. Johnson and Jackson determined the boundary condition involving the slip velocity between the granular material and the bounding surface by equating the tangential force per unit area exerted by the particles on the boundary surface to the corresponding stress within the granular material that is close to the boundary. The force per unit area on the boundary is made up of the frictional and collisional contributions. By making use of Coulomb's law we can express the tangential frictional component of stress as $N_f \tan\delta$, where N_f is the normal rate independent component of stress and δ is the angle of friction between the surface and the granular material. The rate of momentum transfer to the unit area of the surface by collisions is the product of the collision frequency per particle $(3T)^{1/2}/s$, the average tangential momentum transferred per collision $\phi' \pi \rho_s d^3 u_{sl}/6$, and the number of particles adjacent to a unit area of surface $1/a_c$. In these expressions s represents the average distance between the boundary and the surface of an adjacent particle, a_c is the average boundary area per particle, ρ_p is the mass density of the particle, $u_{sl} = u - u_{wall}$ is the wall slip velocity and u_{wall} is the wall velocity. The value of the wall specularity coeffcient φ′ depends on the large scale roughness of the wall and varies from zero for perfectly smooth walls and specular collisions to unity for perfectly diffuse collisions and rough walls. We can express s and a_c as

$$s = d_p\left[\left(\frac{\nu_{\max}}{\nu}\right)^{1/3}-1\right] \tag{24}$$

and

$$a_c = d_p^2\left(\frac{\nu_{\max}}{\nu}\right)^{2/3} \tag{25}$$

Equating the sum of the frictional and collisional stresses at the boundary to the component of the interior bulk stress in the direction of u_{sl} yields

$$\frac{u_{sl}\,.(\sigma_f+\sigma_c).n}{|u_{sl}|}+\frac{\varphi'\sqrt{3}\,\pi\,\rho_p\,\nu\sqrt{T}\,|u_{sl}|}{6\,\nu_{\max}\left[1-(\nu/\nu_{\max})^{1/3}\right]} + N_f\,\tan\delta = 0 \tag{26}$$

For the present case of two-dimensional flow, and using Equation (6) to eliminate T, Equation (26) leads to the following expression for the slip velocity

$$|u_{sl}| = \left[\frac{6\nu_{\max}R\left[1-(\nu/\nu_{\max})^{1/3}\right]}{\varphi' d_p\sqrt{3}\,\pi\,\rho_p\,\nu(du/dy)}\right]. \left[N_f\left(\tan\varphi_f-\tan\delta\right)+\sigma_{yy}\,\tan\varphi_d\right] \tag{27}$$

where values in the right hand side of Equation (27) are evaluated at y=0, and N_f is the quasi-static normal stress. Note that when $\nu \to \nu_{max}$, the slip velocity $u_{sl} \to 0$. According to Johnson and Jackson (1987), the value of the specularity coefficient is $\varphi' \approx 0.6$ for a rough bed.

RESULTS

Some typical numerical calculations are presented here for the following parameter values s:

$$\alpha = 2,\ \nu_{\min} = 0.4,\ \nu_{\max} = 0.6,$$
$$\varphi_f = 15^0,\ \varphi_d = 23^0,\ and\ R = 0.7.$$

The choice of those values is guided, in a general sense, by previous analyses and experimental studies, such as those of Savage (1979), Johnson and Jackson (1987), Vallance (1994), and Hanes and Walton (2000).

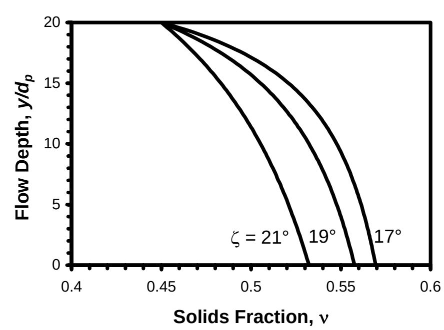

Figure 3a: Profiles of solids volume fraction for different slopes.

The role of the slope is illustrated by conducting runs for three values for the angle ζ of 17^0, 19^0 and 21^0. The resulting distributions of solids volume fraction and velocities are shown in Figures 3a and 3b.

The distributions of the solids volume fraction start with the minimum value at the surface and increase downwards. As expected, the values of solids fraction decrease with increasing slope. The results, shown in Figure 3b, correspond to a no-slip condition at the bottom boundary. The values of the velocities increase with increasing slope. Moreover, the resulting shapes of the velocity distributions are convex; i.e. they display higher gradients near the bottom. That shape of the velocity distribution may be the result of the formulation of the dynamic component of the stress, particularly its dependence on solids volume fraction. Therefore, runs were carried out with a modified form of the function $k_2(\nu)$, different from that given by Equation (21). The following expression was used

$$k_2 = \frac{0.002}{\left(\nu_{\max} - \nu\right)^3} \tag{28}$$

Equation (28) implies that the dependence of $k_2(\nu)$ on ν is stronger than that according to Equation (21). The resulting distributions of solids volume fraction are not affected by the new formula. The shapes of the velocity profiles, however, show inflection points, particularly for the smaller slopes (see Fig. 4).

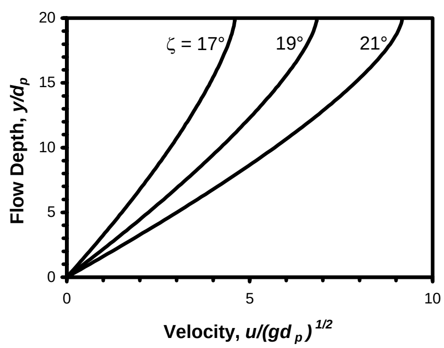

Figure 3b: Velocity profiles for different slopes.

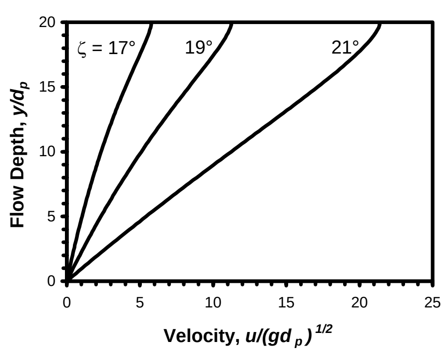

Figure 4: Velocity distributions obtained using a modified expression for $k_2(\nu)$, given by Equation (28).

At present, there is no definite experimental evidence to determine the appropriate shape of velocity distributions. However, some experiments (e.g. Hanes and Walton 2000) indicate that velocity distributions may have inflection points (with maximum gradients near mid-height of the flow). Such measurements by necessity are done at sidewalls, which may affect the velocity distributions. The present results, however, show that the velocity distributions can be adjusted through the choice of the expression for $k_2(\nu)$, which may be adjusted as new experimental evidence becomes available.

Slip velocities at the bottom boundary are included in the computation using Equation (27). Computations are done for a slope of 21^0, and using values for the friction angle δ of 20^0, 15^0, and 10^0. The corresponding values of the specularity coefficient φ' for the three slopes are 0.6, 0.1, and 0.05, respectively. Those values are of the same order used by Johnson and Jackson (1987). There are no specific data, however, to make more precise choices. The resulting velocity distributions are shown in Figure 5. The results display a plausible trend of increasing slip velocity as the friction angle decreases.

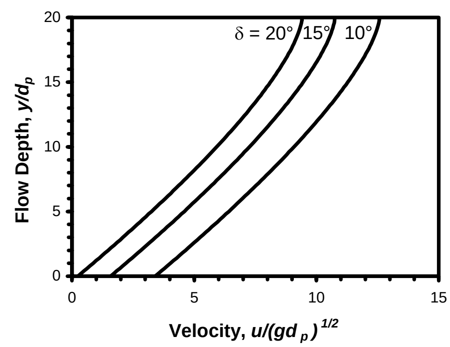

Figure 5: Velocity profiles showing slip velocity at the boundary.

The present analysis is largely based on the assumption of a constant value for the parameter *R*. Larcher (2002) measured values ranging from 0.4 to unity, although the experiments were done using particles submerged in water. At present, Particle-Image-Velocimetry (PIV) measurements are underway (N. Jesuthasan, personal communication). Preliminary results from those measurements suggest that the value of *R* is roughly one. According to the present analysis the value of *R* affects the velocity profile, but has no influence on that of the solids volume fraction. Figure 6 shows the velocity profiles for a range of values of *R*. The results show that the value of *R* affects the magnitude of the velocity. We note that the parameter *R* accounts for the dissipative properties of the material, which depend on factors such as particle sizes, shapes, and the restitution coefficient. The value of *R* can thus be used as an empirical parameter to tune the model to the particular type of flow under consideration.

The experimental data of Hanes and Walton (2000) give values of mean velocities and solids volume fraction that can be compared to the present calculations. They presented such values for slopes of 23.4^0 and 21.2^0. They also found that steady uniform flow could be achieved between slopes of 16^0 and 24^0. Therefore, those values are used for the frictional and dynamic angles of internal friction in the model, ϕ_f and ϕ_d, respectively. The results of the model are compared to the experimental values in Table 1.

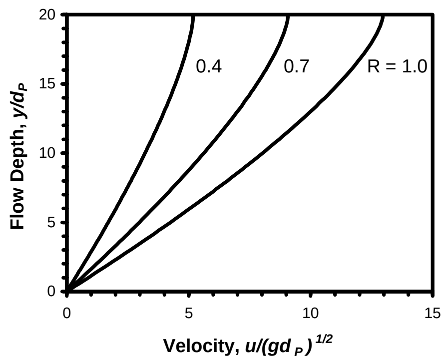

Figure 6: Velocity profiles for different values of the parameter *R*.

	Slope 23.4^0	
	Experiments	Model
Mean velocity, $\bar{u}\Big/\sqrt{g\ d_p}$	3.83	3.71
Mean solids volume fraction, $\bar{\nu}$	0.4	0.48
	Slope 21.2^0	
	Experiments	Model
Mean velocity, $\bar{u}\Big/\sqrt{g\ d_p}$	3.08	3.00
Mean solids volume fraction, $\bar{\nu}$	0.48	0.49

Table 1: Comparison of model predictions with the experiments of Hanes and Walton (2000).

The above comparison shows very good agreement for mean velocities, and somewhat of a less degree for the solids fraction values. The good agreement in Table 1, however, might be fortuitous and have resulted from the particular choice of parameters. For example, changing the value of the parameter, α from 2.0 to 1.0 gives the following results. For slope of 23.4^0, the mean velocity and solids volume fraction were 4.85 and 0.47, respectively. For slope of 21.2^0, the corresponding values were 2.52 and 0.48. The corresponding flow depth to particle diameter ratios, h/d_p were 11.3 and 9.7.

Comparisons with the experimental data presented by Vallance (1994) are also done here. The data were adapted from measurements of Johnson (1987) and presented as mean velocities versus flow depth. Figure 7 shows model results superimposed on the data points. Calculations were done using the following values for the angles of friction: $\varphi_f=15^0$, $\varphi_d=23^0$, and $\delta=15^0$. The value of the specularity coefficient φ' was 0.1. The comparison indicates that model predictions are of the same order as the measurements. The model also displays similar trends to the experiments of increasing velocity with increasing flow height and slope. The experiments, however, show a maximum value of mean velocity at a particular flow depth for each slope. With increasing flow depth, after that point, the mean velocity decreases. A possible reason for that behaviour is the effect of sidewall friction. As flow depth increases, the ratio of flow depth to channel width increases, and the role of that friction is likely to be more pronounced. The present two-dimensional analysis cannot capture that effect. Three-dimensional simulations are needed to clarify that issue.

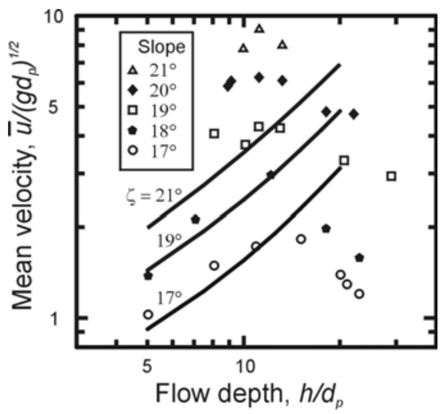

Figure 7: Numerical results of mean velocity versus flow height compared to data presented by Vallance (1994).

CONCLUSION

The present paper has focused on the development and compilation of simple forms for constitutive equations that can be used for the calculation of granular flows. These constitutive equations are intended to be used for the prediction of flows down inclined chutes. Various approximations and simplifications based on the geometric restrictions and the particular characteristics associated with such channelized flows have been made. A major part of the paper is concerned with the various contributions to the stresses, the dynamic contributions made up of the kinetic and the collisional parts, and the quasistatic contribution arising from the enduring contacts generated as particles override one another.

The dynamic stress contributions are based on previous granular flow kinetic theory results and simplifications that result from the assumption that the Savage-Jeffrey parameter *R* is a constant (*R* is proportional to the shear rate divided by the square root of the granular temperature). The assumption that $R \approx$ constant, seems plausible for certain chute flows and furthermore eliminates the need to make use of the particle fluctuation energy equation (sometimes called the pseudo-thermal energy equation). The assumption of a constant *R* probably breaks down when there is a significant pseudo-thermal energy flux divergence over the depth of the flow. Such a breakdown might arise when there is significant pseudo-thermal flux introduced or removed at a boundary such as the bed. Expressions for stresses in both two-dimensional and three-dimensional flow fields are presented. Bed boundary conditions and bed slip velocities are discussed.

A solution for steady uniform flow was next obtained. The results were verified through comparisons to a few available experimental measurements. The comparisons indicate that predicted velocities and flow rates are of the same order as the experiments. Also trends concerning the role of various factors, such as slope of the chute and friction of the bed, were in agreement with the experiments.

ACKNOWLEGEMENT

We are indebted to Anne Collins, CHC/NRC, for kind help with the analysis. This work was sponsored by the Climate Change Action Plan (CCAP) 2000, through the project on Granular Multiphase Flow. We would also like to acknowledge Kim Smith (OERD) for his support and interest in this project.

REFERENCES

ANDERSON, P.C. and JACKSON, R., (1992), “A comparison of the solutions of some proposed equations of motion of granular materials for fully developed flow down an inclined plane”, *J Fluid Mech.*, **241**, 145-168.

HANES, D.M. and WALTON, O.R., (2000), “Simulations and physical measurements of glass spheres flowing down a bumpy incline,” *Powder Technology*, **109**, 133-144.

JOHNSON, P.C., (1987), “Frictional-collisional equations of motion for particulate flows with application to chutes and shear cells,” PhD Thesis, Princeton University, p. 381.

JOHNSON, P.C. and JACKSON, R. (1987), “Frictional-collisional constitutive relations for granular materials with application to plane shearing,” *J Fluid Mech.*, **176**, 67-93.

JOHNSON, P.C., NOTT, P. and JACKSON, R. (1990), “Frictional-collisional equations of motion for particulate flows and their application to chutes”, *J. Fluid Mech*., **210**, 501-535.

LARCHER, M. (2002), “Vertical structure of high-concentration liquid-granular flows”, PhD Thesis, Universita Degali Studi Di Padova, Italy, December 2002, p.201.

LUN, C.K.K., SAVAGE, S.B., JEFFREY, D.J. and CHEPURNIY, N. (1984), “Kinetic theories for granular flow: inelastic particles in Couette flow and slightly inelastic particles in general flow field”, *J Fluid Mech.*, **140**, 223-256.

LUN, C.K.K. and SAVAGE, S.B. (1986), “The effects of an impact velocity dependent coefficient of restitution on stresses developed by sheared granular materials”, *Acta Mechanica*, **63**, 15-44.

LUN, C.K.K. and SAVAGE, S.B. (1987), “A simple kinetic theory for granular flow of rough, inelastic spherical particles,” *J Applied Mech.*, **54**, 47-53.

SAVAGE, S.B. and JEFFREY, D.J. (1981), “The stress tensor in a granular flow at high shear rates”, *J Fluid Mech.*, **110**, 255-272.

SAVAGE, S.B. (1979), “Gravity flow of cohesionless granular materials in chutes and channels”, *J Fluid Mech.*, **92**, 53-96.

SYAMLAL, M., ROGERS, W.A. and O’BRIEN, T.J. (1993), “MFIX documentation and theory guide”, DOE/METC-94/1004, NTIS DE94000087. Electronically available from: http://www.mfix.org/documentation/Theory.pdf

VALLANCE, J.W. (1994), “Experimental and field studies related to the behavior of granular mass flows and the characteristics of their deposits,” PhD Thesis, Michigan Technological University, p. 197.

VAN WACHEM, B.G.M., SCHOUTEN, J.C., VAN DEN BLEEK, C.M., KRISHNA, R., and SINCLAIRE, J.L. (2001), “Comparative analysis of CFD models of dense gas-solid systems”, *AIChE Journal*, **47**, 5, 1035-1051.